



Available online at www.sciencedirect.com



Surface Science 548 (2004) 183–186



www.elsevier.com/locate/susc

Reflectance anisotropy of uracil covered Si(0 0 1) surfaces: Ab initio predictions

K. Seino, W.G. Schmidt *

Institut für Festkörpertheorie und Theoretische Optik, Friedrich-Schiller-Universität Jena, Max-Wien-Platz 1, 07743 Jena, Germany

Received 15 August 2003; accepted for publication 5 November 2003

Abstract

Reflectance anisotropy spectra (RAS) for energetically favored models of uracil covered Si(0 0 1) surfaces have been calculated within the independent particle approximation. While for low coverages mainly an attenuation of the features typical for the clean surface is found, the calculations predict the appearance of new peaks for higher coverages, suggesting the usage of RAS for the analysis of organic/inorganic interfaces.

© 2003 Elsevier B.V. All rights reserved.

Keywords: Reflection spectroscopy; Density functional calculations; Semiconducting surfaces; Silicon

Organic functionalization of semiconductors has become important for the development of new semiconductor-based devices. The physical and chemical properties of hybrid organic/inorganic materials depend crucially on the structural and chemical details of the interface. Techniques like electron diffraction or scanning tunneling microscopy (STM) give information on the order and symmetry of the organically modified surface [1]. However, they usually do not allow for discriminating between competing bonding scenarios. On the other hand, optical spectroscopies such as reflectance anisotropy spectroscopy (RAS) have been shown to be highly successful in the determination of semiconductor surface structures, see, e.g. Refs. [2,3]. This holds in particular if the

measurements are accompanied by accurate *first-principles* calculations [4,5]. At present, however, there are only very few studies that explore optical anisotropies of organically modified semiconductors (see, e.g., Refs. [6,7]). Here we calculate RAS spectra for several structural models of an organic overlayer on a semiconductor in order to investigate the sensitivity of RAS with respect to the details of the interface bonding.

As model system we have chosen the adsorption of uracil on Si(0 0 1). This system, investigated experimentally by STM and high-resolution electron energy-loss spectroscopy [8], leads to what can be considered a prototypical interface between a polyfunctional organic molecule and a semiconductor surface. The (0 0 1) surface of silicon is the starting point for the fabrication of most microelectronic devices. Uracil ($C_4H_4N_2O_2$) features one $C=C$ double bond, two N–H and two carbonyl groups and may thus bond to the surface in various ways [8,9].

* Corresponding author. Tel.: +49-3641947163; fax: +49-3541947151.

E-mail address: w.g.schmidt@ift0.physik.uni-jena.de (W.G. Schmidt).

The calculations are performed using the Vienna Ab-initio Simulation Package (VASP) implementation [10] of the gradient-corrected [11] density functional theory (DFT-GGA). The electron-ion interaction is described by non-normconserving ultrasoft pseudopotentials [12], allowing for the accurate quantum-mechanical treatment of first-row elements with a relatively small basis set of plane waves. We expand the valence wave functions into plane waves up to an energy cutoff of 25 Ry. This approach has been shown to accurately reproduce the geometry and electronic ground state of pyrimidine and purine bases [13].

The Si(001) surface is modeled with a periodically repeated slab. The supercell consists of 12 atomic Si layers plus uracil molecules adsorbed on both sides and a vacuum region equivalent in thickness to eight atomic layers. All calculations are performed using the calculated Si equilibrium lattice constant of 5.456 Å. The outermost four layers of the slab as well as the adsorbed molecules are allowed to relax. Brillouin zone integrations are performed using sets corresponding to 64 \mathbf{k} -points in the full (1×1) surface Brillouin zone (SBZ).

The optical spectra are determined from all-electron wave functions obtained by the projector-augmented wave (PAW) method [14]. Transition matrix elements have been calculated for \mathbf{k} -point sets corresponding to 256 points in the full SBZ. The slab polarizability is calculated in the independent-particle approximation, i.e., neglecting excitonic and local-field effects. A scissors operator approach has been used to account for the band-gap underestimation of 0.5 eV for bulk Si due to the neglect of self-energy effects within the DFT. RAS spectra have been calculated from the slab polarizability according to the scheme devised by Del Sole and co-workers [15,16]. Calculations for smaller systems [17,18] have shown that many-body effects alter RAS spectra quantitatively rather than qualitatively, because RAS spectra are difference spectra, which are furthermore normalized to the bulk dielectric function. Therefore, calculations within the independent-particle approximation reliably reproduce experimental data for a wide range of semiconductors [19].

From previous total-energy calculations [9] in conjunction with experimental work [8] it was

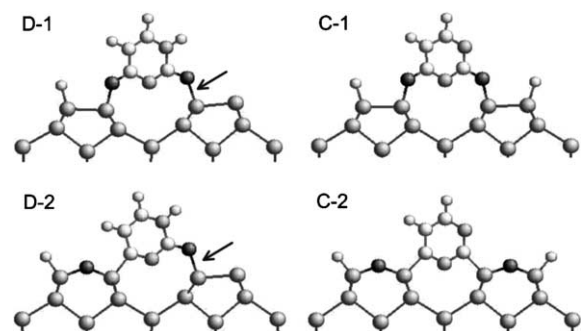


Fig. 1. Uracil/Si(001) adsorption configurations. White, grey, dark grey, black, and small symbols indicate C, N, Si, O, and H atoms, respectively. Dative bonds are marked by arrows.

concluded that uracil adsorption on Si(001) is likely to result in the dimer bridging configurations shown in Fig. 1. Starting from a dative-bonded configuration, where uracil is attached to the electron-poor “down” Si dimer atom via one carbonyl group, a relative low energy barrier of about 0.3 eV needs to be overcome for hydrogen dissociation, molecular rotation around the surface normal and tilting towards the neighboring Si dimer [9]. This leads to the configurations where uracil is partially dative (D-1 in Fig. 1) or completely covalently (C-1) bonded to the Si surface bridging two Si dimer rows, respectively. The latter structure requires in addition a dienol to keto-enol transition of the gas-phase uracil or during the tilting process. The direct pathway from D-1 to C-1 via diffusion of hydrogen is hindered by a relative high barrier energy of more than 1 eV. A similar energy barrier of more than 1 eV is required for oxygen insertion into Si dimers, leading to the very favorable interface configurations D-2 and C-2 [9]. The calculated adsorption energies of the models D-1, C-1, D-2, and C-2 amount to 2.77, 3.66, 3.78, and 5.27 eV, respectively. The dative bond (see arrows in Fig. 1) in the structures D-1 and D-2 occurs between the electron-rich uracil carbonyl group and the electron-poor atom of the clean Si dimer. It is about 0.1 Å longer than the corresponding covalent Si–O bond [9].

In order to verify the accuracy of our RAS calculations we first studied the optical response of the clean, $c(4 \times 2)$ reconstructed Si(001) surface.

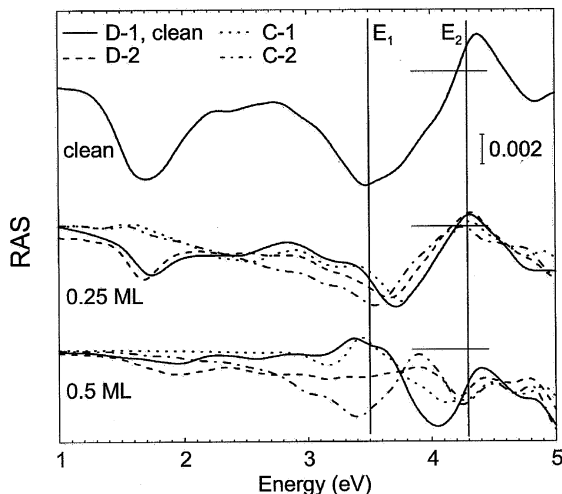


Fig. 2. RAS spectra [$\text{Re}\{(r_{[110]} - r_{[110]})/\langle r \rangle\}$] calculated for the uracil/Si(001) adsorption configurations shown in Fig. 1 are compared with results for the clean surface. Thin lines are used to indicate the calculated positions of the E_1 and E_2 critical point energies as well as the positions of zero optical anisotropy.

The calculated spectrum is shown in upper part of Fig. 2. A strong, dimer-state related minimum occurs at 1.7 eV. An additional minimum/maximum structure slightly below/above the E_1/E_2 critical point energies of bulk Si at 3.5/4.3 eV results from surface-modified bulk states. The calculated results are in excellent agreement with the data measured on highly oriented, single-domain Si(001) surfaces prepared by electro-migration [20]. Experimental spectra obtained for vicinal Si(001) surfaces [21,22] showed an additional feature at 3.0 eV that is due to surface steps [23,24].

The reflectance anisotropy of the Si(001) surface changes upon adsorption of uracil. A coverage of 0.25 ML, defined here to correspond to one adsorbed molecule per (4×2) surface unit cell, leads to a complete cancellation or a reduction by a factor of two of the 1.7 eV RAS feature for the covalently or partially dative-bonded adsorption geometries, respectively. This is to be expected. Covalently or dative-bonded interface geometries lead to complete or partial removal of Si-dimer related surface states from the energy region of the fundamental gap, respectively. Also the neighbor-

ing dimers, while not directly involved in the bonding to the molecule, are affected. We calculate a reduction of the dimer tilting by 1–2° and 2–3° for the Si dimers next to a dative or covalently bonded uracil molecule, respectively. Less drastic are the changes of optical anisotropies at higher energies. Here we basically observe an attenuation of the RAS peaks for all structures. These peaks are mainly due to microscopic electric fields induced by the anisotropy of the electron potential in the surface region [25]. All bonding geometries considered in the present work are characterized by a substantial, largely lateral charge transfer. Depending on the adsorption configurations, we calculate values between 10 and 15 electrons per adsorbed molecule. Therefore, the surface potential of all bonding configurations is affected, resulting in changes of the E_1/E_2 RAS features that are less bonding specific than the low-energy transitions directly related to Si surface states.

The modification of the Si(001) RAS signal increases with increasing uracil coverage. For the half-monolayer case all Si surface atoms of the C-1 and C-2 models are covalently bonded. Accordingly, these models show only very weak optical anisotropies below the onset of the bulk transitions at the E_1 critical point energy of Si. In case of D-1 and D-2, two Si surface dangling bonds per (4×2) unit cell remain and there is a very weak RAS feature at 1.7 eV. The RAS features between about 3.0 and 4.5 eV are very structure dependent. A sign reversal compared to the clean Si(001) surface is found for the D-1 and C-1 models: positive and negative anisotropies are predicted for photon energies close to the E_1 and E_2 critical point energies, respectively. A similar behavior has been found experimentally [26] and computationally [18] for the structurally similar monohydride Si(001) surface. The RAS signals for the models D-2 and C-2, where oxygen is inserted into the Si dimers, differ appreciably from the spectra predicted for D-1 and C-1. D-2 shows nearly no variation of the RAS signal below the E_2 critical point energy and C-2 features negative anisotropy peaks at both E_1 and E_2 . Unfortunately, the manifold of electronic transitions, mainly between bulk-like Si states that contribute to the optical anisotropies at E_1 and E_2 , prevents a simple

interpretation of the high-energy RAS features in terms of bond polarizabilities [27].

In summary, we predict for low uracil coverage the attenuation of the optical anisotropy of the Si(001) surface. For high coverages, i.e. if every Si dimer is involved in the interface bonding, changes of the RAS signal are calculated that are strongly structure dependent and may thus allow for discriminating between different interface bonding scenarios. Our calculations suggest the measurement of the surface optical anisotropy as a complementary tool to explore the structural details of organic/inorganic interfaces.

Acknowledgements

Grants of computer time from the Leibniz-Rechenzentrum München, the Höchstleistungs-Rechenzentrum Stuttgart and the John von Neumann-Institut Jülich are gratefully acknowledged. We thank the Deutsche Forschungsgemeinschaft for financial support (SCHM-1361/6).

References

- [1] R.A. Wolkow, Annu. Rev. Phys. Chem. 50 (1999) 413.
- [2] D.E. Aspnes, Solid State Commun. 101 (1997) 85.
- [3] W. Richter, J.T. Zettler, Appl. Surf. Sci. 101 (1996) 465.
- [4] W. Lu, W.G. Schmidt, E.L. Briggs, J. Bernholc, Phys. Rev. Lett. 85 (2000) 4381.
- [5] W.G. Schmidt, P.H. Hahn, F. Bechstedt, N. Esser, P. Vogt, A. Wange, W. Richter, Phys. Rev. Lett. 90 (2003) 126101.
- [6] A. Sassella, A. Borghesi, F. Meinardi, R. Tubono, M. Gurioli, C. Botta, W. Porzio, G. Barbarella, Phys. Rev. B 62 (2000) 11170.
- [7] A.M. Paraian, U. Rossow, S. Park, G. Salvan, M. Friedrich, T.U. Kampen, D.R.T. Zahn, J. Vac. Sci. Technol. B 19 (2001) 1658.
- [8] A. Lopez, Q. Chen, N.V. Richardson, Surf. Interface Anal. 33 (2002) 441.
- [9] K. Seino, W.G. Schmidt, M. Preuss, F. Bechstedt, J. Phys. Chem. B 107 (2003) 5031.
- [10] G. Kresse, J. Furthmüller, Comp. Mater. Sci. 6 (1996) 15.
- [11] J.P. Perdew, J.A. Chevary, S.H. Vosko, K.A. Jackson, M.R. Pederson, D.J. Singh, C. Fiolhais, Phys. Rev. B 46 (1992) 6671.
- [12] J. Furthmüller, P. Käckell, F. Bechstedt, G. Kresse, Phys. Rev. B 61 (2000) 4576.
- [13] M. Preuss, W.G. Schmidt, K. Seino, J. Furthmüller, F. Bechstedt, J. Comp. Chem., in press.
- [14] B. Adolph, J. Furthmüller, F. Bechstedt, Phys. Rev. B 63 (2001) 125108.
- [15] R. Del Sole, Solid State Commun. 37 (1981) 537.
- [16] F. Manghi, R. Del Sole, A. Selloni, E. Molinari, Phys. Rev. B 41 (1990) 9935.
- [17] P.H. Hahn, W.G. Schmidt, F. Bechstedt, Phys. Rev. Lett. 88 (2002) 016402.
- [18] W.G. Schmidt, S. Glutsch, P.H. Hahn, F. Bechstedt, Phys. Rev. B 67 (2003) 085307.
- [19] W.G. Schmidt, F. Bechstedt, J. Bernholc, J. Vac. Sci. Technol. B 18 (2000) 2215.
- [20] R. Shiota, J. van der Weide, Phys. Rev. B 57 (1998) R6823.
- [21] L. Kipp, D.K. Biegelsen, J.E. Northrup, L.-E. Swartz, R.D. Bringans, Phys. Rev. Lett. 76 (1996) 2810.
- [22] T. Yasuda, L. Mantese, U. Rossow, D.E. Aspnes, Phys. Rev. Lett. 74 (1995) 3431.
- [23] S.G. Jaloviar, J.-L. Lin, F. Liu, V. Zielasek, L. McCaughan, M.G. Lagally, Phys. Rev. Lett. 82 (1999) 791.
- [24] W.G. Schmidt, F. Bechstedt, J. Bernholc, Phys. Rev. B 63 (2001) 045322.
- [25] W. Schmidt, K. Seino, P. Hahn, F. Bechstedt, W. Lu, S. Wang, J. Bernholc, Thin Solid Films, submitted for publication.
- [26] R. Shiota, J. van der Weide, Appl. Surf. Sci. 130–132 (1998) 266.
- [27] W.G. Schmidt, N. Esser, A.M. Frisch, P. Vogt, J. Bernholc, F. Bechstedt, M. Zorn, T. Hannappel, S. Visbeck, F. Willig, W. Richter, Phys. Rev. B 61 (2000) R16335.